

# Slack-chain mooring configuration analysis of a floating wave energy converter

Pedro C. Vicente<sup>1</sup>, António F. de O. Falcão<sup>1</sup> and Paulo A.P. Justino<sup>2</sup>

<sup>1</sup>IDMEC, Instituto Superior Técnico, Technical University of Lisbon, Lisboa, Portugal

<sup>2</sup>Laboratório Nacional de Energia e Geologia, Lisboa, Portugal

## Abstract

In this paper, different mooring configurations with slack chain mooring lines of a floating point absorber are analyzed, with or without additional sinkers or floaters. The slack mooring cables are approximately modelled as catenary lines in a quasi-static analysis in a time-domain model that takes into account the non-linearities of the system introduced by the non linear mooring forces and that affect the motions of the converter. Numerical results for the motions, mooring demands and also absorbed power by the converter, are presented for the different mooring configurations, for a system consisting of a hemispherical buoy in regular waves and assuming a liner power take-off system.

## Introduction

Floating point absorbers, as any floating object, are subject to drift forces due to waves, currents and wind, and have to be kept on station by moorings. Their mooring design has an important requirement, associated to the fact that, for a wave energy converter, the mooring connections may interact with its oscillations, which may significantly modify its energy absorption. It is therefore important to investigate what might be the most suitable mooring design according to the converter specifications and taking into account the demands placed on the moorings in order to assure its survivability.

A wide range of different options exists for the mooring design and configuration. They can be either single slack chain catenary cables or taut synthetic mooring lines or a composite of several cable segments and can also have additional sinkers or floaters. Different configurations will represent different displacements from the equilibrium position for the converter and load demands on the moorings and also of course different installation and maintenance costs. Slack chain catenary lines rely on their weight to provide the necessary horizontal restoring force and although they induce some vertically downward force they allow for systems with a lower stiffness than the ones with taut synthetic lines.

## Mathematical Model

We consider a hemispherical buoy, moored to the bottom by catenary lines, as shown in plan view in Fig. 1, for different configurations, a single line (I-red), with an intermediary floater at a lower (II-light green) or higher (III-dark green) position, with two different floaters at different depths (IV-light blue), with a floater and weight (V-dark blue) and with a floater at the sea surface (VI-orange). Cables in the same configuration are placed to the right side of the buoy.

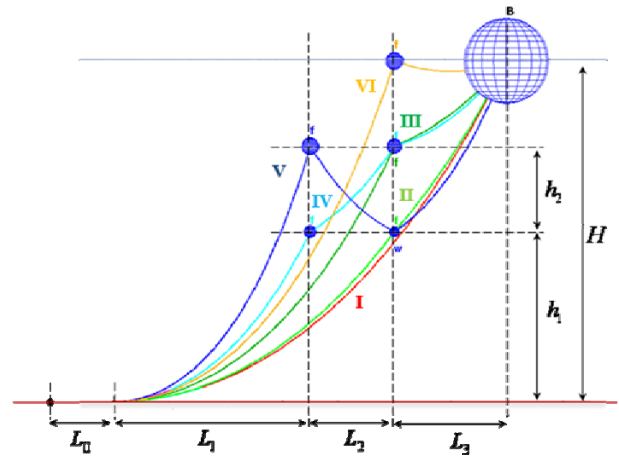


Figure 1- Plane view of the mooring configurations.

In the absence of waves, we assume that the centre of the buoy lies on the free-surface plane, a vertical distance  $H$  from the bottom of the sea, and an initial horizontal distance  $L_0 + L_1 + L_2 + L_3$  from the anchor point on the bottom, where  $L_0$  is the length of the cable that initially lays on the seabed and  $L_1, L_2, L_3$  are the horizontal lengths of the hanging parts of the cable and  $h_1, h_2$  the vertical ones, at which, in some of the configurations, floaters or weights are placed (see Fig. 1).

In this analysis the slack mooring cables are approximately modelled as catenary lines, are assumed inelastic and their dynamic effects (namely cable inertia and viscous drag forces) are ignored but not the submerged cable weight per unit length  $W$ , which depends on the cable material used (chain, wire, fibre) (see [1]). The classical catenary equations([2]) apply, which can be written as

$$Z = \left( \frac{T_H}{W} \right) \cosh \left( \frac{D}{T_H/W} + \alpha \right) + \beta, \quad (1)$$

$$s = \left( \frac{T_H}{W} \right) \sinh \left( \frac{D}{T_H/W} + \alpha \right) + \gamma, \quad (2)$$

$$T = T_H \cosh\left(\frac{D}{T_H/W} + \alpha\right), \quad (3)$$

$$T_V = T_H \sinh\left(\frac{D}{T_H/W} + \alpha\right). \quad (4)$$

Here,  $D$  and  $Z$  are the horizontal and vertical coordinates of the cable point with respect to the lowest point of the catenary (where the cable departs from the bottom);  $\alpha$ ,  $\beta$  and  $\gamma$  are constants determined from boundary conditions;  $s$  is the length of the catenary-shaped part of the cable;  $T$  is the tension force on the cable, and  $T_H$  and  $T_V$  its horizontal and vertical components;  $W$  is the cable weight (minus buoyancy force) per unit length.

The boundary conditions at the point of seabed contact are  $s=0$ ,  $D=0$ ,  $Z=0$ ,  $dZ/dD=0$  and at the buoy  $D=L_1+L_2+L_3$  and  $Z=H$ . At the intermediary points where the additional bodies are placed, the boundary conditions are such that

$$\left.\frac{dZ}{dD}\right|^+ - \left.\frac{dZ}{dD}\right|^- = \frac{P_b}{T_H}, \quad (5)$$

where  $P_b$  is a force downwards (if the body is denser than water) or upwards (if the body is less dense than water) and that is equal to the difference between the body weight and its buoyancy force

$$P_b = m_b g - v_b \rho_0 g = v_b (\rho_b - \rho_0) g. \quad (6)$$

From these boundary conditions it is possible to calculate, for the initial equilibrium position, the initial horizontal cable tension  $T_H$  and after that  $T_V$  and  $T$ . It is also possible to calculate the necessary body radius of which floater or weight and the hanging cable length  $s$ , which in turn allows to calculate the necessary cable length  $l$  of each section ( $l=s+L_0$  for the cable connected to the anchor point on the bottom and  $l=s$  for the remaining). It is also easy to calculate the initial horizontal and vertical mooring tensions, applied to each intermediary body,  $R_H$  and  $R_V$ , respectively.

Since, in calm sea, the centre of the hemispherical buoy (of radius  $a$ ) is supposed to lie on the free-surface plane, the buoy mass  $m$  must be

$$m = \frac{2}{3} \pi a^3 \rho - \frac{1}{g} 2T_V. \quad (7)$$

Note that, since the buoy centre is assumed to lie on the free-surface horizontal plane in static conditions, the mass  $m$  of the moored buoy slightly varies with each mooring configuration parameters.

### Time Domain Analysis

The buoy and bodies acted upon by the waves and mooring lines are made to oscillate in heave and horizontally. The displacements of their centre from

their mean position is defined by the coordinates  $(x_j, z_j)$  with  $j=B$  for the buoy, and  $j=b$  for the intermediary bodies and where  $x$  is the horizontal coordinate, and  $z$  is a vertical coordinate pointing upwards.

The dynamic equations for the buoy are then

$$(m + A_{\infty x}) \ddot{x}_B(t) + \int_{-\infty}^t L_x(t-\tau) \ddot{x}_B(\tau) d\tau = f_{dx_B} \cos\theta - T_{X,A} - T_{X,B}, \quad (8)$$

$$(m + A_{\infty z}) \ddot{z}_B(t) + \rho g S z_B(t) + \int_{-\infty}^t L_z(t-\tau) \ddot{z}_B(\tau) d\tau = f_{dz_B} - C \dot{z}_B - (T_{Z,A} + T_{Z,B}) + (2T_V). \quad (9)$$

Here,  $A_{\infty u}$  ( $u=x, z$ ) are the limiting values of the added masses  $A_u(\omega)$  for  $\omega=\infty$ . For a hemispherical floater, it is  $A_{\infty z} = \mu/2$  and  $A_{\infty x} = 0.2732\mu$ , where  $\mu = 2\pi a^3 \rho/3$  (see [3]).  $f_{dx}$  and  $f_{dz}$  are the horizontal ( $x$ ) and vertical ( $z$ ) components of the wave excitation force on the buoys (see [4]). The power take-off system (PTO) of each floating converter is assumed to consist of a simple linear damper activated by the buoy heaving motion. The vertical force it produces on the buoy is  $-C \dot{z}_B$ . Finally,  $S = \pi a^2$ .

The convolution integrals in Eqs. (8-9) represent the memory effect in the radiation forces. Their kernels can be written as

$$L_u(t) = \frac{2}{\pi} \int_{-\infty}^t \frac{B_u(\omega)}{\omega} \sin \omega t d\omega \quad (u=x, z). \quad (10)$$

They decay rapidly and may be neglected after a few tens of seconds, which means the infinite interval of integration in Eqs. (8-9) may be replaced by a finite one in the numerical calculations (a 20s interval was adopted as sufficient). The integral-differential equations (8-9) were numerically integrated from given initial values of  $x$ ,  $z$ ,  $\dot{x}$  and  $\dot{z}$ , with an integration time step of 0.05 s.

$B_u(\omega)$  ( $u=x, z$ ) are the frequency-dependent hydrodynamic coefficients of radiation damping concerning the horizontal (subscript  $x$ ) and heave (subscript  $z$ ) oscillation modes of the spherical buoys.

$T_V$  is as already mentioned the initial vertical cable tension applied at the buoy, at equilibrium position. The time varying values of the mooring forces  $T_{X,v}$  and  $T_{Z,v}$  on each cable  $v=A, B$  on the left and right side of the buoy are calculated based on the position of each body ( $j=b$ ) and the tension applied to it ( $F=R$ ) or buoy ( $j=B$ ) and tension applied ( $F=T$ ), at each instant of time, and considering the cable length  $l$  defined for the static position and the similar catenary equations

$$Z + z_j = \left( \frac{F_{X,v}}{W} \right) \cosh \left( \frac{D \pm x_j}{F_{X,v}/W} + \alpha \right) + \beta, \quad (11)$$

$$s = \left( \frac{F_{X,v}}{W} \right) \sinh \left( \frac{D \pm x_j}{F_{X,v}/W} + \alpha \right) + \gamma. \quad (12)$$

The plus or minus sign is used according to the cable considered is on the right or left side of the buoy.

The intermediary bodies are subject to the pulling forces of the mooring lines, their own weight, the buoyancy force and the hydrodynamic forces on them. Similar dynamic equations to the ones of the buoy apply

$$(m_b + A_{\infty bh}) \ddot{x}_b(t) + \int_{-\infty}^t L_{4h}(t-\tau) \ddot{x}_b(t) d\tau = f_{dbx} \cos \theta - R_{bX,A} - R_{bX,B} \quad (13)$$

$$(m_b + A_{\infty bz}) \ddot{z}_b(t) + \int_{-\infty}^t L_{bz}(t-\tau) \ddot{z}_b(t) d\tau = f_{dbz} + (R_{bZ,A} + R_{bZ,B}) - (2R_V) \quad (14)$$

The kernels of the convolution integrals  $L_{bu}$  ( $u = x, z$ ) are calculated as before, considering  $B_{bu}(\omega)$  ( $u = x, z$ ) as the hydrodynamic coefficients of radiation damping of the bodies.  $f_{dbx}$  and  $f_{dbz}$  are the horizontal and vertical components of the wave excitation force on the bodies. In this case, the effects of the wave radiation and diffraction induced by the buoy upon the bodies were neglected. For the added mass  $A_{\infty bu}$  ( $u = x, z$ ), we take the added mass of an accelerating sphere in an unbounded fluid (see e.g. [5])  $A_{bx} = A_{bz} = (2/3) \rho \pi a_b^3$ .

## Numerical Results

We set  $\rho = 1025 \text{ kg.m}^{-3}$  (sea water density) and  $g = 9.8 \text{ ms}^{-2}$ . The intermediary floaters are spheres of density  $\rho_b = 50 \text{ kg.m}^{-3}$  and the weights spheres of density  $\rho_b = 2000 \text{ kg.m}^{-3}$  (typical of concrete). The bodies submergence (except for the floater in VI) is assumed to be sufficient for the excitation force and the radiation damping on them to be neglected, i.e. we set  $B_{bx} = B_{bz} = 0$  and  $f_{dbx} = f_{dbz} = 0$ .

In all cases for which results are shown here, it is  $a = 7.5 \text{ m}$ ,  $H = 60 \text{ m}$ ,  $L_0 = 0.65 \times (L_1 + L_2 + L_3)$ ,  $L_1 = 35 \text{ m}$ ,  $L_2 = 15 \text{ m}$ ,  $L_3 = 20 \text{ m}$ ,  $h_1 = 30 \text{ m}$ ,  $h_2 = 45 \text{ m}$  and  $C = 251.1 \text{ kN/(m/s)}$ .

In all configurations except VI, a value for the submerged cable weight of  $W = 1520 \text{ N/m}$  was used, adequate for example for a 90mm thick chain cable (see [3]). In VI a value of  $W = 6000 \text{ N/m}$  (180mm thick chain) was used in order to assure the cable exerted enough horizontal restoring force to keep the

buoy in place. The adopted value of  $C = 251.1 \text{ kN/(m/s)}$  is obtained from defining  $C = B$ , and is the one that allows maximum wave energy absorption by an isolated unmoored hemispherical heaving buoy, at resonance frequency (see e.g. [4]).

Table 1 shows for the different configurations analyzed and for the proposed configuration parameters:  $a_{b1}$  and  $a_{b2}$  – first and second (from anchor point) radius of the mooring bodies (floaters or weight) and  $l_T$  – total mooring cable length. As can be seen the average size of the additional bodies is about 1m radius, slightly more for the floater that lays on the sea surface (VI). In terms of required total cable length for the mooring configurations, differences mainly appear for the floater-weight (V) and floater at sea surface (VI) configurations, requiring slightly longer cables.

**Table 1 – Resulting parameters for the proposed mooring configurations.**

	I	II	III	IV	V	VI
$a_{b1}(\text{m})$	-	0.7	1.3	1.1	1.5	2.4
$a_{b2}(\text{m})$	-	-	-	1.0	0.9	-
$l_T(\text{m})$	97	97	96	95	118	103

In regular waves the excitation force components are assumed to be simple-harmonic functions of time and so we may write  $\{f_{dx}, f_{dz}\} = \text{Re}(\{F_{dx}, F_{dz}\} e^{i\omega t})$ , where the complex amplitudes  $F_{dx}$  and  $F_{dz}$  are proportional to the amplitude  $A_w$  of the incident wave. The moduli of  $F_{dx}$  and  $F_{dz}$  may be written as  $\{|F_{dx}|, |F_{dz}|\} = \{\Gamma_x A_w, \Gamma_z A_w\}$ , where  $\Gamma_x(\omega)$  and  $\Gamma_z(\omega)$  are (real positive) excitation force coefficients.

Deep water was assumed for the hydrodynamic coefficients of added mass, radiation damping and excitation force. The frequency dependent numerical values were obtained with the aid of the boundary element code WAMIT, for the radiation damping coefficients  $B_u(\omega)$  and the absolute value  $\Gamma_u(\omega)$  and phase  $\arg(F_{dz}(\omega)/F_{dx}(\omega))$  of the excitation forces coefficients, for the floating hemispheres, oscillating horizontally and vertically ( $u = x, z$ ).

Some numerical results are illustrated in Fig. 2 and Table 1, for regular waves of  $A_w = 1 \text{ m}$  and  $T = 10 \text{ s}$  for a 5min computational simulation.

The spectral analyses of the heave and surge oscillations, shows a peak at 0.1 Hz for both heave and surge, corresponding to the wave frequency, and a 2<sup>nd</sup> low frequency peak ( $f_{lp}$ ) for surge only.

Fig.2 shows the phase diagrams for surge, for each mooring configuration, where the complex curve characteristic of a non-simple-harmonic time variation can be seen, revealing the nonlinearity effects on the horizontal motions and forces, as well the influence of the low frequency peak in each configuration.

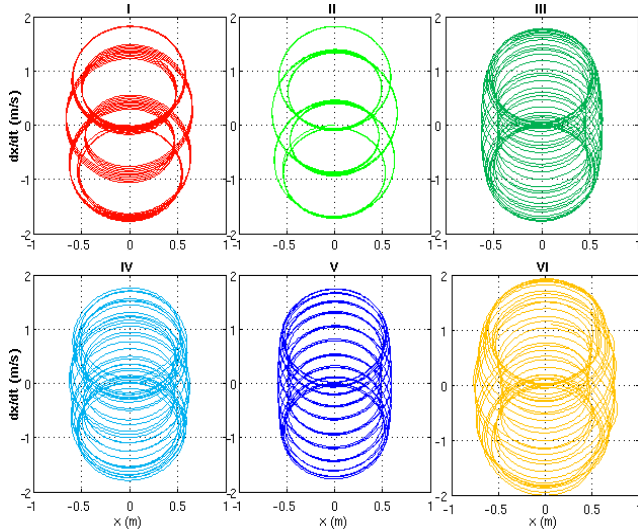


**Figure 2 – Phase diagrams for surge velocities in each mooring configuration.**

Table 2 shows for the different configurations analyzed:  $z_{rms}$  – heave motion root mean square,  $x_{Max}$  – maximum surge motion,  $f_{lp}$  – horizontal motion low frequency peak,  $T_{avg}$  – average mooring force at the buoy,  $T_{Max}$  – maximum mooring force on the whole mooring cable,  $P_{avg}$  – average absorbed power and  $q^*$  – power coefficient between the power absorbed by the moored and unmoored converter.

**Table 2 - Results in buoy motion, mooring forces and absorbed power for the different configurations for regular waves of  $A_w = 1$  m,  $T = 10$  s.**

	I	II	III	IV	V	VI
$z_{rms}$ (m)	0.54	0.55	0.55	0.55	0.55	0.55
$x_{Max}$ (m)	1.83	1.82	1.78	1.76	1.74	1.93
$f_{lp}$ (mHz)	17.1	17.1	14.6	14.6	9.7	24.2
$T_{avg}$ (kN)	165	151	78	62	79	180
$T_{Max}$ (kN)	182	168	134	97	165	560
$P_{avg}$ (kW)	37.1	37.2	37.9	38.1	37.8	37.4
$q^*$	0.96	0.97	0.98	0.99	0.98	0.98

It can be seen that the influence in terms of heave average displacement is negligible and in terms of maximum horizontal motion and resonance frequency is not very significant.

The more visible distinctions are in terms of average mooring tension at the buoy, which are smaller in the III, IV and V configurations, and of maximum mooring tension on the cable, smaller in IV and quite larger in the VI configuration.

Finally, in terms of average power absorbed and power coefficient, the differences are quite small, with IV appearing very slightly more beneficial.

## Conclusions

A theoretical analysis of the wave-induced heave and surge oscillations of a slack moored wave energy converter was presented. Different configurations are analyzed of slack chain mooring lines, with or without additional floaters or weights. A time-domain analysis was applied to investigate the nonlinear effects of the mooring forces.

Numerical results were obtained for a hemispherical buoy whose PTO consists of a linear spring and a linear damper, and focusing on the amplitude of the motion of the converters, tension demands on the moorings and power absorbed for each configuration.

Slack chain catenary lines rely on their weight to provide the necessary horizontal restoring force and although they induce some vertically downward force, they were found not to affect significantly the power absorption in any of the proposed configurations.

The nonlinearities were found to affect much more markedly the horizontal oscillations: even in regular waves, they exhibit significantly non-simple-harmonic time-variations. This nonlinear behaviour derives from the nonlinear relationship between cable tension and buoy displacements.

The different configurations proposed revealed only slight differences in term of maximum horizontal displacement and power absorbed, but significant differences were found in terms of average and maximum tensions on the mooring cables.

## References

- [1] I. Johanning, G.H. Smith, J. Wolfram. Mooring design approach for wave energy converters. Proc. Inst. Mech. Eng. Part M-J. Eng. Marit. Environ., vol. 220, p. 159-174, 2006.
- [2] R.J. Smith, C.J. MacFarlane. Statics of a three component mooring line. Ocean Eng., vol. 28, p. 899-914, 2001.
- [3] Hulme, A., 1982, "The Wave Forces Acting on a Floating Hemisphere Undergoing Forced Periodic Oscillations," J. Fluid Mech., 121, pp. 443-463.
- [4] J. Falnes. Ocean Waves and Oscillating Systems. Cambridge University Press, Cambridge, 2002.
- [5] J. Lighthill. An Informal Introduction to Theoretical Fluid Mechanics. Oxford University Press, Oxford, 1986.